Supplementary Information for: Reimagining Interface Processing in Solid-State Batteries via Electrochemical Flash Sintering

Authors:

Riku Fukada[a], Claire V. Colin[a], Timothée Fabre[b], Marlu César Steil[b], Renaud Bouchet[b], Maria Diaz-Lopez[a]*

Affiliations :

[a]Institut Néel, CNRS, Université Grenoble-Alpes, CNRS, F-38042 Grenoble, France

[b]Université Grenoble Alpes, Université Savoie Mont Blanc, CNRS, Grenoble INP, LEPMI, 38000 Grenoble, France

*Email: maria.diaz-lopez@neel.cnrs.fr

Table of contents:

Supplementary Figure

Supplementary Tables

Supplementary Figures

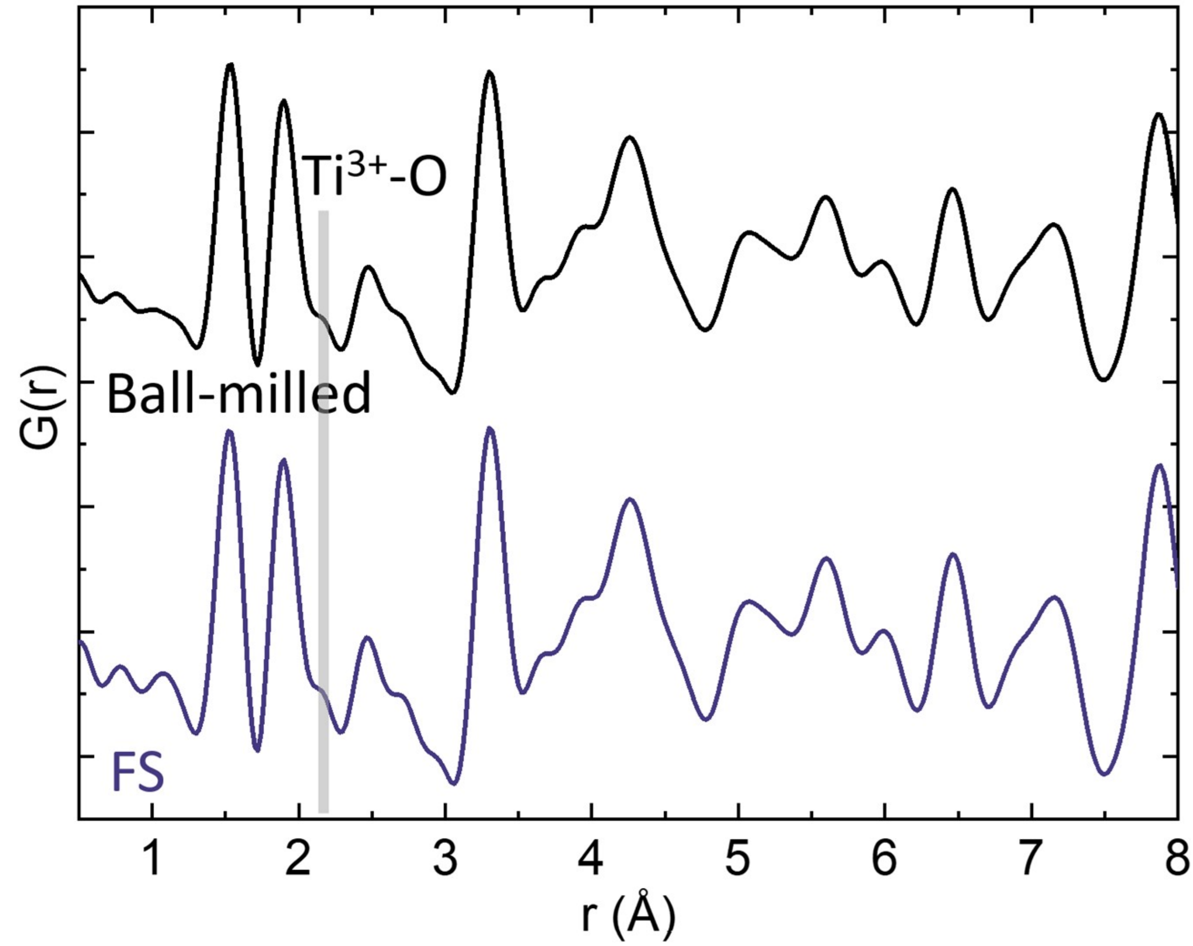

Figure S1. PDF of the unsintered LATP precursor (LATP Ball Milled) and FSed LATP (LATP-4A-100kHz) showing the presence of a Ti^{3+}- O peak alongside the Ti^{4+}/Al^{3+}–O, indicating that reduced titanium species are already present before flash sintering.

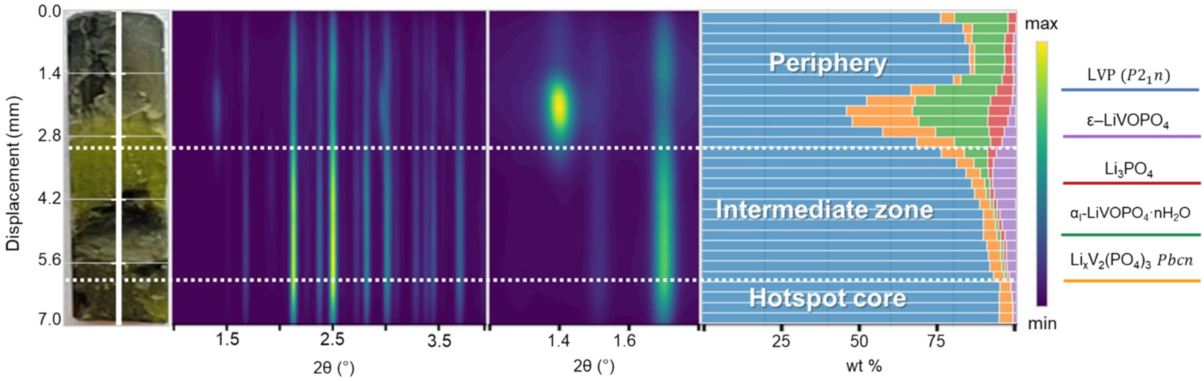

Figure S2. Cross-section measurement of LVP-7.5A-1kHz: Optical images (left), 1D X-ray diffraction heatmaps across the pellet thickness (center), phase quantification by Rietveld refinement (right).

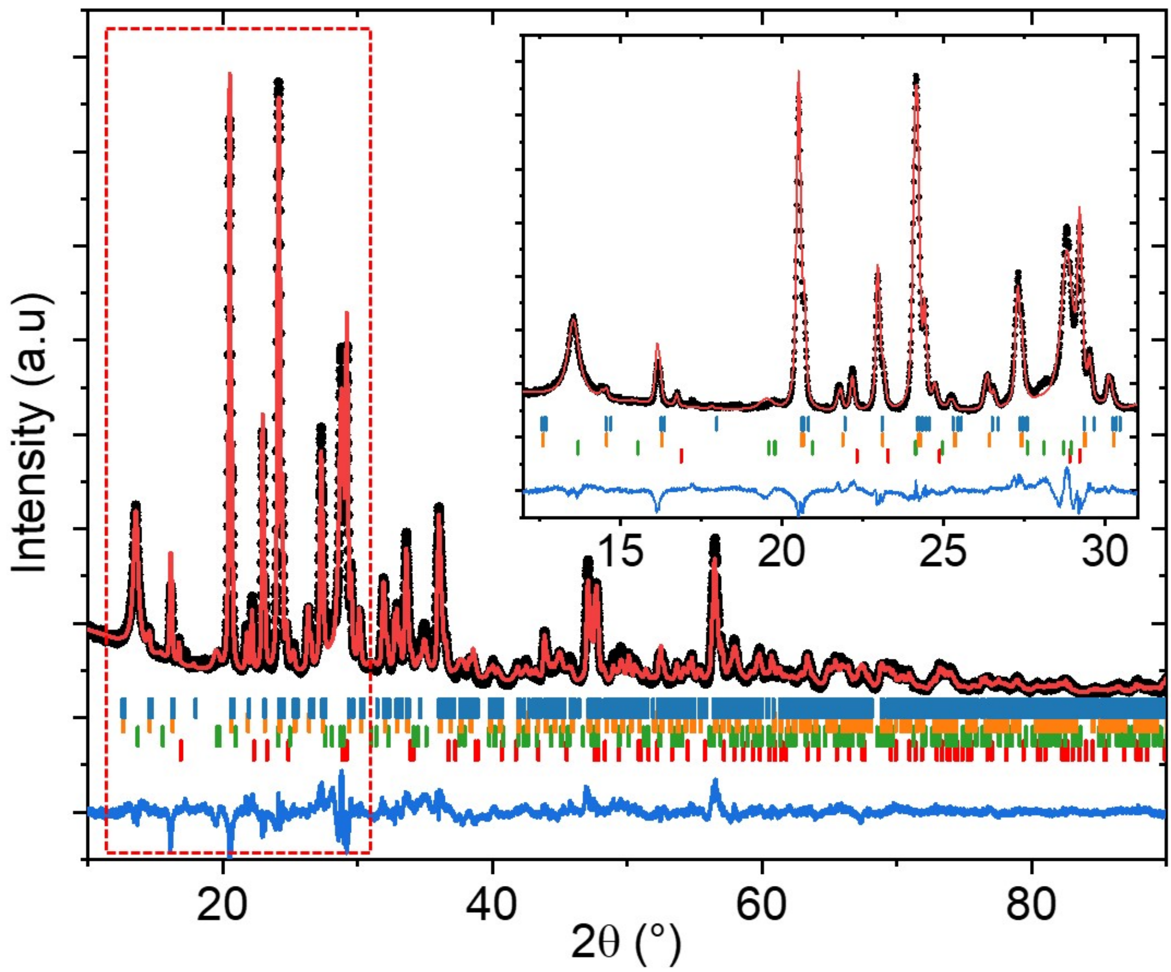

Figure S3. Rietveld refinement of the peripheral zone of LVP sintered at 6 A/cm². Preferential orientation was observed for α_I-$LiVOPO_4$ and accounted for using a spherical harmonics (4th order) correction. The refinement resulted in R_{wp}=8.64% , R_{exp}=2.89%, and a goodness-of-fit (GOF) value of 2.99.

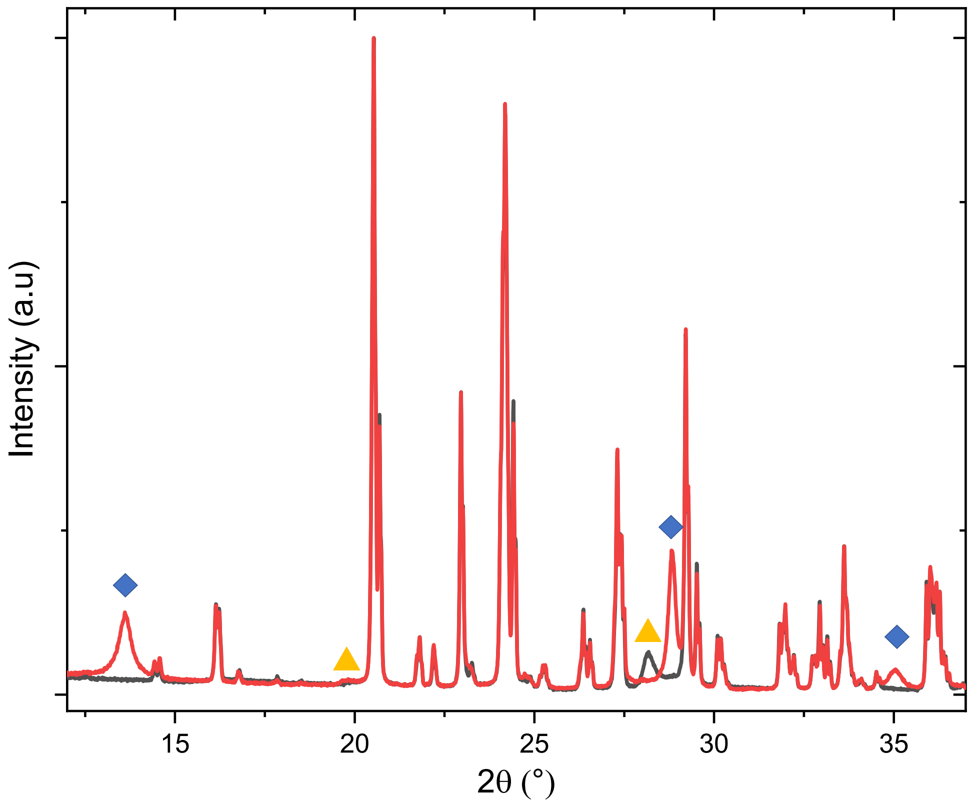

Figure S4. (red) XRD analysis of LVP processed at 800°C under vacuum, changes after extended exposure to ambient atmosphere (black) after leaving under high vacuum for 1 day.

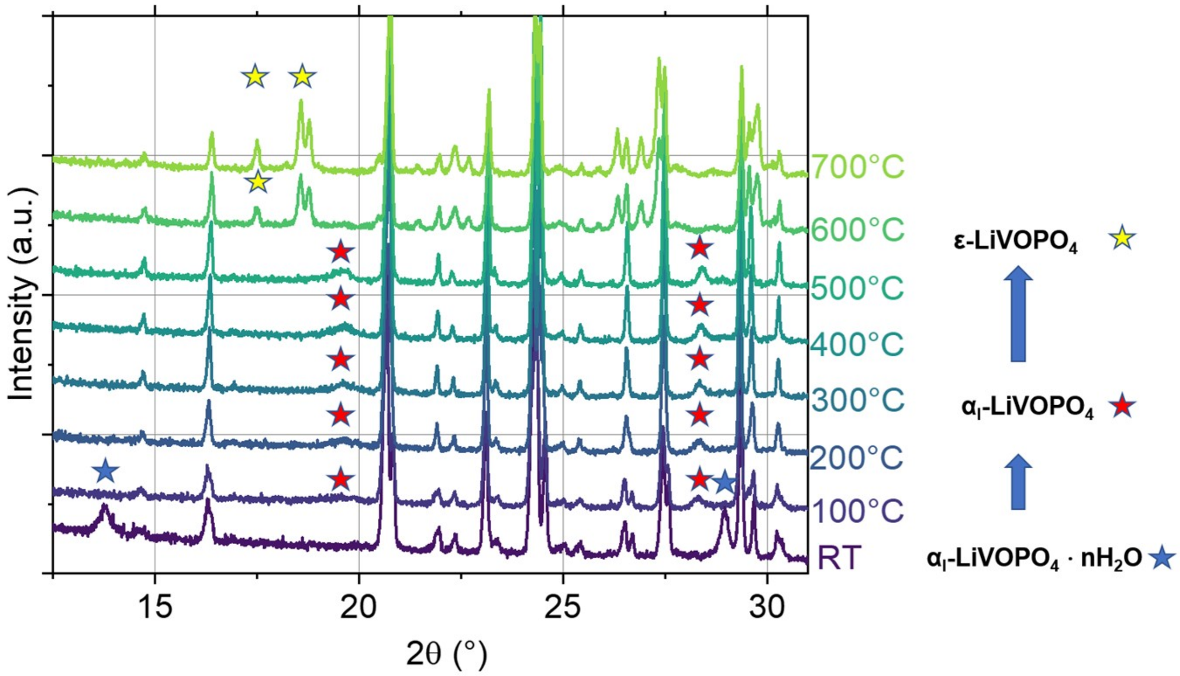

Figure S5. Variable temperature X-ray diffraction from RT to 700°C.

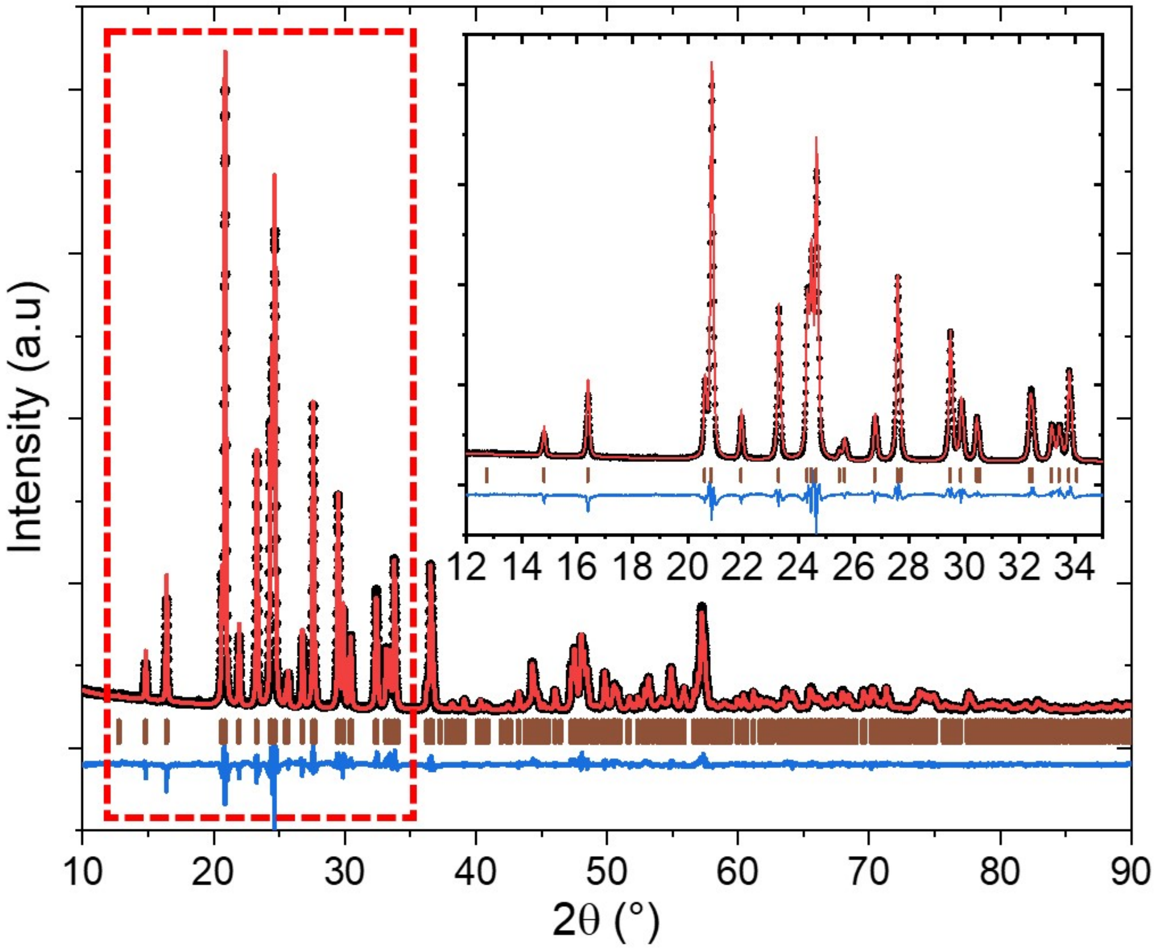

Figure S6. Rietveld refinement of the composite powder sintered at 800°C under Ar. The refinement resulted in R_{wp}=7.04% , R_{exp}=2.79%, and a GOF value of 2.53.

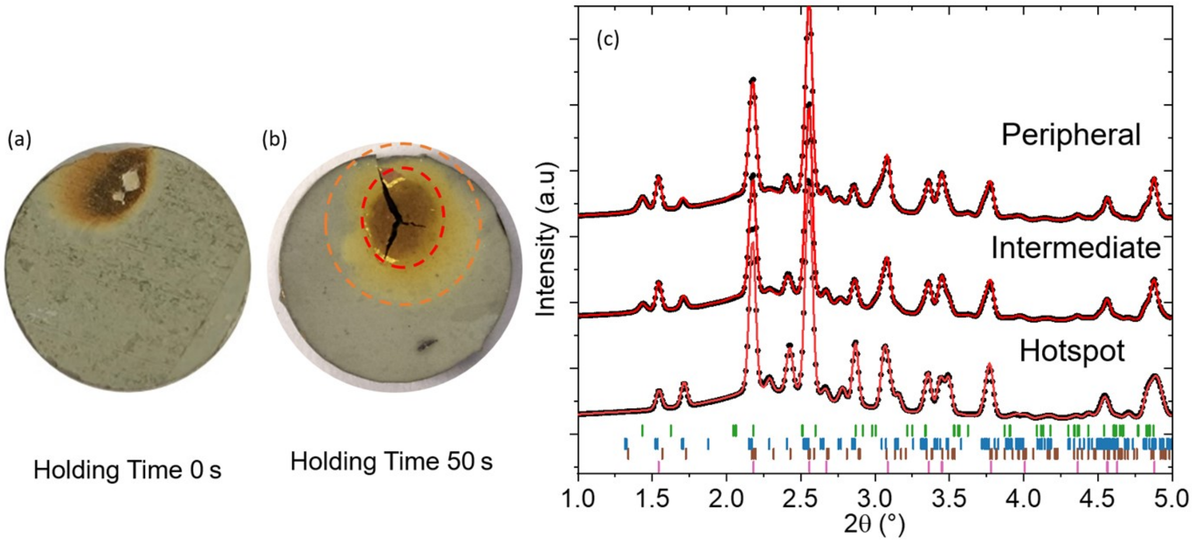

Figure S7. Composite-6A-1kHz-0s (a) and Composite-6A-1kHz-50s (b) Composite-6A-1kHz-50s was divided into three zones. Rietveld refinement of synchrotron XRD data of the resulting three zones (c) Vertical lines indicate the Bragg position of each phase: (blue) LVP, (pink) LATP, (brown) LATVP, (green) α_I-$LiVOPO_4 \cdot nH_2O$

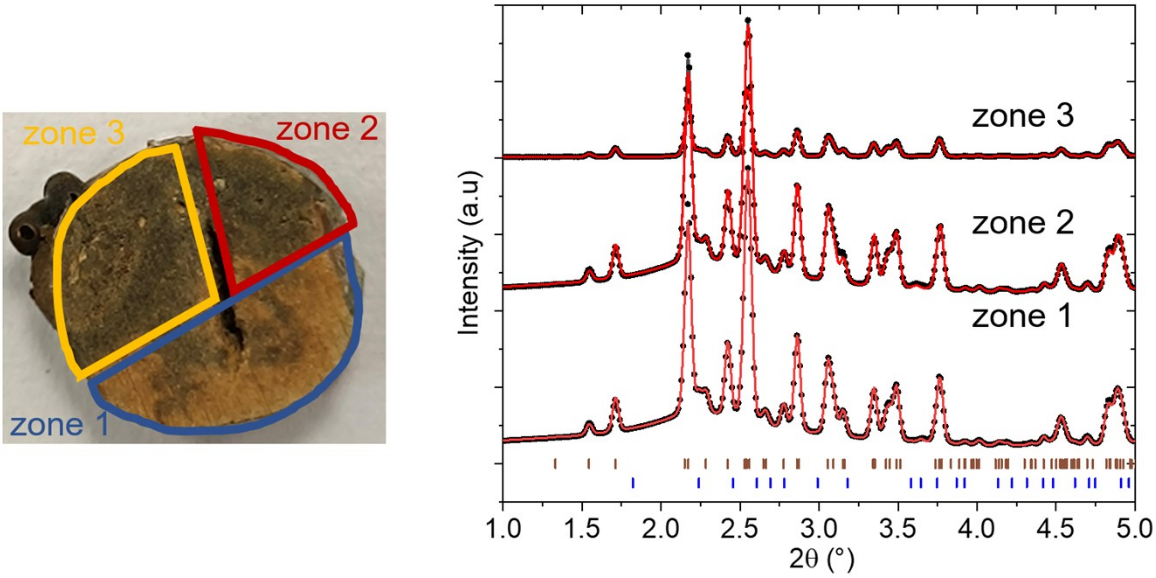

Figure S8. Composite-6A-200kHz pellet was divided into three zones. Rietveld refinement of synchrotron XRD data of resulting three zones (Left) Vertical lines indicate the Bragg position of each phase: (blue) AlPO, and (brown) LATVP

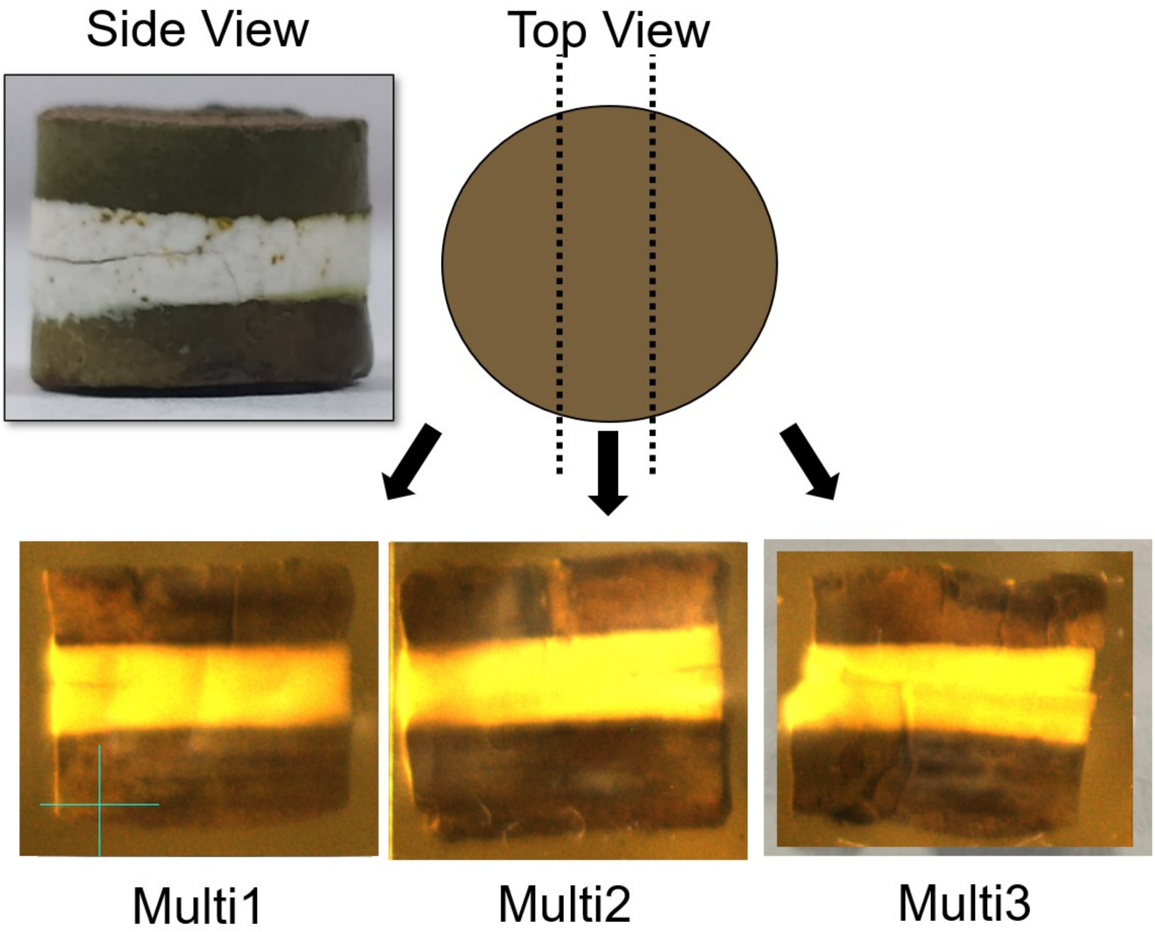

Figure S9. Overview of the Flash-Sintered ML Pellet. The pellet was sectioned into three parts: densified side (Multi1), less densified (Multi3), and the center part (Multi2).

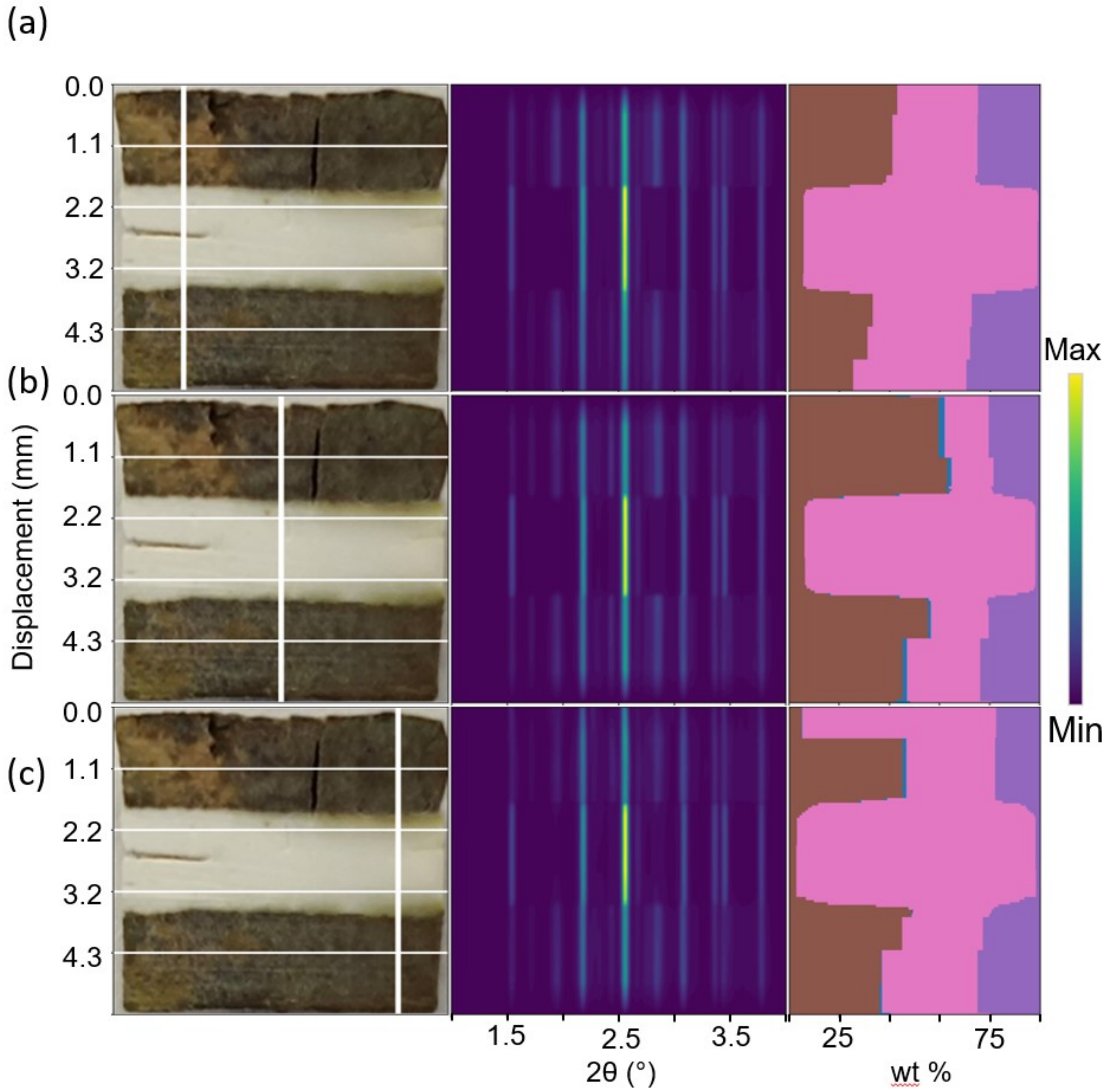

Figure S10. Structural evolution across Multi1

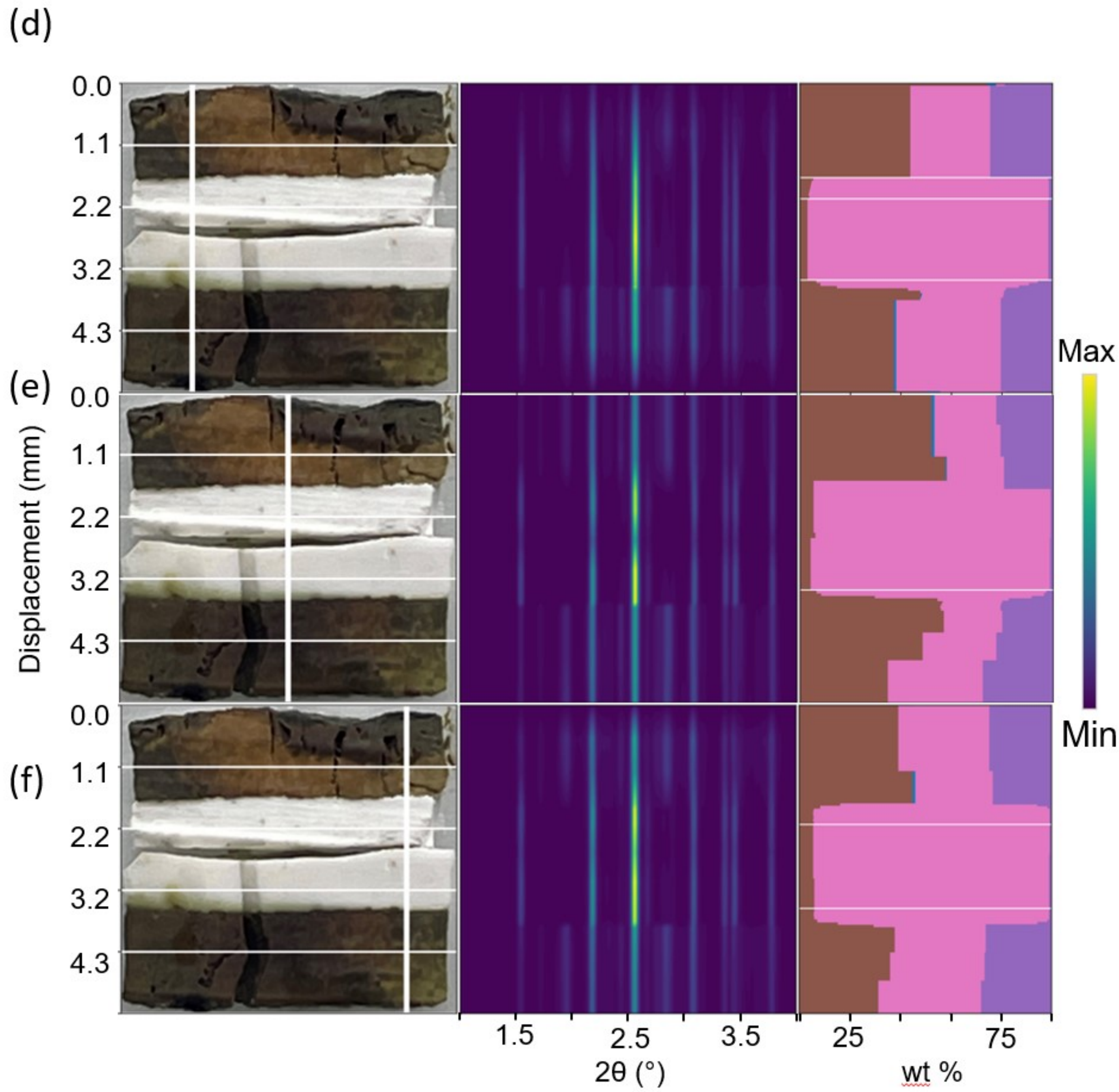

Figure S11. Structural evolution across Multi3. The pellets fractured after the experiment. This image was reconstructed by taping the fragments together. Experimental data were recorded before breakage.

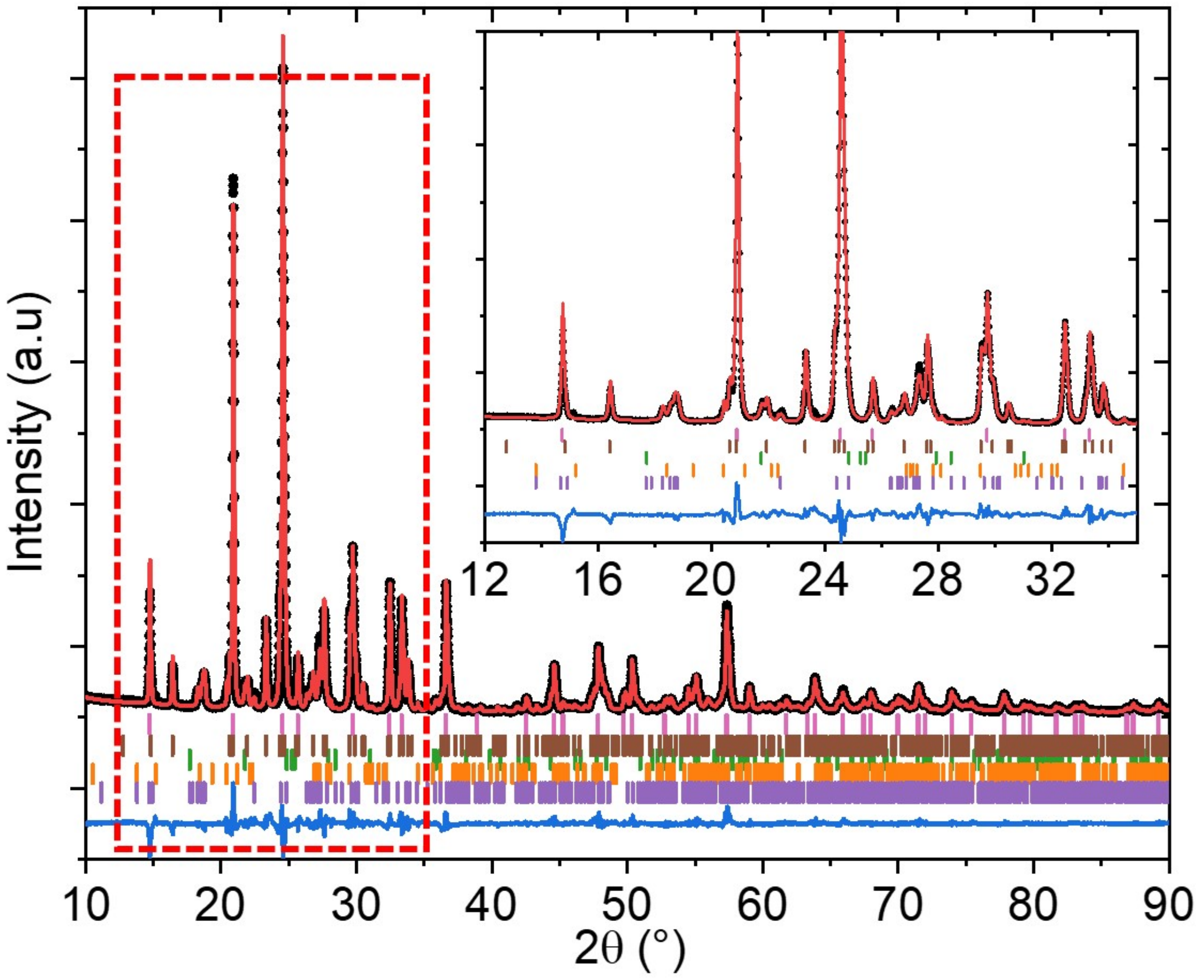

Figure S12. Rietveld Refinement of densified region of ML: Vertical lines indicate the Bragg position of each phase: (pink) LATP, (brown) LATVP, (green) $AlPO_4$, (orange) $Li_4P_2O_7$, and (purple) ε–$LiVOPO_4$

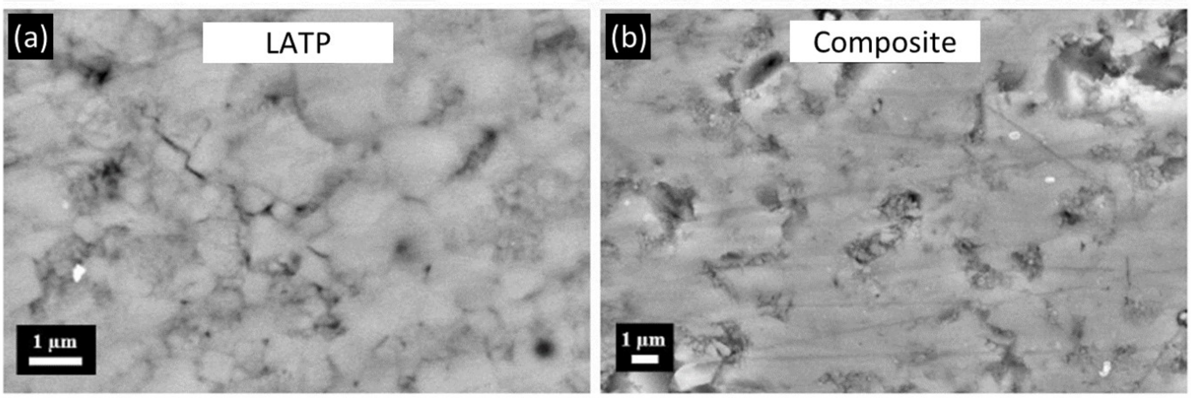

Figure S13. High-magnification SEM-BSD images of the sintered multilayer. These images support the densification and structural cohesion of individual LATP and composite layers discussed in the main text (see Section Monolithic Processing of LVP|LATP|LVP Multilayer Architectures).

Figure S14. Images of LATP pellets after flash sintering: LATP-4A-100kHz (left, Au electrodes) and LATP-300V-500kHz (right, Pt electrodes).. The observed melting and redistribution of the Au/Pt electrodes, including metallic globules trapped within the ceramic matrix, indicate localized overheating during flash and support the occurrence of temperatures above the melting points of Au (1064 ºC) and Pt (1768 ºC).

Supplementary Tables

Table S 1. Experimental parameters and sample acronyms

Sample ID	Composition	Applied V (V/cm)	Incubation *T* (°C)	Frequency (kHz)	Applied *I* (A/cm²)	Hold *t* (s)
LVP Ball Milled	LVP	LVP Ball-milled powder				
LVP-CS-Ar	LVP	Conventionally sintered pellet under Ar (980°C 3h)				
LVP-FS	LVP	100	300	1	6	25
LVP-CS-Ar+3%H2	LVP	Conventionally sintered under Ar+3%H_2				
LVP-2A-1kHz	LVP	100	300	1	2	50
LVP-6A-1kHz	LVP	100	300	1	6	50
LVP-9A-1kHz	LVP	100	300	1	9	5
LVP-6A-100kHz	LVP	100	300	100	6	50
LVP-7.5A-1kHz	LVP	100	300	1	7.5	50
LATP Ball Milled	LATP	LATP Ball-milled powder				
LATP-CS-Air	LATP	Conventionally sintered pellet under air (1000°C)				
LATP-4A-100kHz	LATP	200	250	100	4	20
LATP-300V-500kHz	LATP	300	370	500	3	27
Composite Ball Milled	LATP:LVP (6:4)	LATP:LVP-Ball Milled (BM)				
Composite CS	LATP:LVP (6:4)	Conventionally sintered pellet under Ar (800°C 3h) Conventionally sintered pellet under Ar (750°C 3h) Conventionally sintered pellet under Ar (700°C 3h)				
Composite-6A-1kHz-50s	LATP:LVP (6:4)	100	300	1	6	50
Composite-6A-1kHz-0s	LATP:LVP (6:4)	100	300	1	6	0
Composite-6A-300kHz	LATP:LVP (6:4)	100	300	300	I_{set} = 6 I_{exp} = 3	50
Composite-6A-200kHz	LATP:LVP (6:4)	100	300	200	6	50
Composite-6A-100kHz	LATP:LVP (6:4)	100	300	100	6	50
Multilayer	LVP–LATP | LATP | LVP–LATP	200	485	1	6	50

Table S 2. Summary of refinement parameters of the partially melted zone of LATP sintered at 500 kHz. Preferential orientation was observed for LATP and accounted for using a spherical harmonics (6th order) correction. The refinement resulted in R_{wp}=7.13

Phase	$Li_{1.4}Al_{0.4}Ti_{1.6}(PO_4)_3$	$AlPO_4$	$LiTiOPO_4$	Li_3PO_4
a (Å)	6.81(2)	8.5006(14)	6.1172	7.37(2)
b (Å)	7.57(2)	8.5006(14)	5.2503	6.421(17)
c (Å)	7.210(17)	20.887(5)	4.8955	7.22(3)
α (°)	90	90	90	90
β (°)	90	90	90	90
γ (°)	90	120	90	90
Volume ($Å^3$)	372.0(19)	1307.1(5)	157.23	342(2)
Space Group	C2221	R-3c	Pmn21	Pnma
Weight %	88.77	6.27	2.88	2.08

Table S 3. Summary of refinement parameters.

Phase	a_I-$LiVOPO_4$ nH_2O	Li_3PO_4	$Li_3V_2(PO_4)_3$ - gamma phase	$Li_3V_2(PO_4)_3$
a (Å)	8.984(2)	6.1172(12)	12.1547(10)	8.6145(5)
b (Å)	8.982(2)	5.2503(9)	8.5983(7)	8.5975(5)
c (Å)	12.932(2)	4.8956(8)	8.6259(7)	12.0468(6)
α (°)	90	90	90	90
β (°)	90	90	90	90.585(4)
γ (°)	90	90	90	90
Volume (Å³)	1043.5(4)	157.23(5)	901.49(13)	892.18(8)
Space Group	Cmca	Pmn21	Pbcn	P21/n
Weight %	25.1	7.25	28.41	39.24

Table S 4. Refinement Parameters of LATVP model: composition of LATVP was refined by fixing the vanadium composition to 0.384, resulting with estimated composition of $Li_2Al_{0.15}V_{0.77}Ti_{1.08}(PO_4)_3$ (theoretical composition $Li_{2.02}Al_{0.24}V_{0.77}Ti_{0.99}(PO_4)_3$)

Label	Element	Multiplicity	Frac_X	Frac_Y	Frac_Z	Occupancy	B_iso
Li_1	Li	8	0.285	0.270	0.317	1	4
V_1	V+3	8	0.25427(19)	0.46464(10)	0.11225(8)	0.384	0.38(3)
Ti_1	Ti+4	8	0.25427(19)	0.46464(10)	0.11225(8)	0.542(6)	0.38(3)
A l_1	Al+3	8	0.25427(19)	0.46464(10)	0.11225(8)	0.074(6)	0.38(3)
P_1	P	8	0.1049(2)	0.10866(19)	0.14685(14)	1	0.55(4)
P_2	P	4	0.0367(3)	0.25	0.5	1	0.55(4)
O_1	O	8	0.4227(4)	0.1051(4)	0.3458(3)	1	0.20(4)
O_2	O	8	0.3253(4)	0.4858(4)	0.2696(3)	1	0.20(4)
O_3	O	8	0.1591(4)	0.0564(4)	0.0296(3)	1	0.20(4)
O_4	O	8	0.4383(3)	0.3604(3)	0.0716(2)	1	0.20(4)
O_5	O	8	0.1454(4)	0.1624(4)	0.4186(2)	1	0.20(4)
O_6	O	8	0.1605(4)	0.2742(4)	0.1785(3)	1	0.20(4)

Table S 5. Summary of Refinement Parameters from Figure 5: Lattice parameter of LATP and LVP model fixed prior to the refinement

Phase	$Li_{1.4}Al_{0.4}Ti_{1.6}(PO_4)_3$	$Li_2(Al,Ti,V)_2(PO_4)_3$	$Li_3V_2(PO_4)_3$
a (Å)	8.497	8.5111(3)	8.616
b (Å)	8.497	8.5979(3)	8.599
c (Å)	20.78	11.9424(3)	12.05
α (°)	90	90	90
β (°)	90	90	90.6
γ (°)	120	90	90
Volume ($Å^3$)	1300	873.92(5)	892.7
Space Group	R-3c	Pbna	P21/n
Weight % (30°C)	58.28	0	41.72
Weight % (700°C)	4.14	86.82	9.04
Weight % (750°C)	0.73	98.61	0.66
Weight % (800°C)	0	100	0

Table S 6. Summary of Refinement Parameters from Figure S7

Phase	a_I-$LiVOPO_4$ nH_2O	$Li_{1.4}Al_{0.4}Ti_{1.6}(PO_4)_3$	$Li_2(Al,Ti,V)_2(PO_4)_3$	$Li_3V_2(PO_4)_3$
a (Å)	9.004(9)	8.4968(3)	8.4982(14)	8.6097(8)
b (Å)	8.974(8)	8.4968(3)	8.5790(14)	8.6012(7)
c (Å)	12.913(6)	20.7948(11)	11.9064(17)	12.0437(13)
α (°)	90	90	90	90
β (°)	90	90	90	90.494(10)
γ (°)	90	120	90	90
Volume (Å³)	1043.3(14)	1300.17(11)	868.1(2)	891.85(15)
Space Group	Cmca	R-3c	Pbna	P21/n
Weight % (Hotspot core)	0	14.71	62.29	23.00
Weight % (Intermediate)	5.36	43.26	17.43	33.96
Weight % (Peripheral)	9.08	51.67	6.22	33.03

Table S 7. Summary of Refinement Parameters from Figure S8

Phase	$AlPO_4$	$Li_2(Al,Ti,V)_2(PO4)_3$
a (Å)	6.883(8)	8.5369(3)
b (Å)	7.546(10)	8.6179(3)
c (Å)	7.106(6)	11.9892(4)
α (°)	90	90
β (°)	90	90
γ (°)	90	90
Volume (Å³)	369.1(7)	882.05(5)
Space Group	C2221	Pbna
Weight % (zone 1)	2.12	97.88
Weight % (zone 2)	1.76	98.24
Weight % (zone 3)	2.45	97.55

Table S 8. Summary of Refinement Parameters from Figure S12.

Phase	$AlPO_4$	LATP	$Li_2(Al,Ti,V)_2(PO_4)_3$	ε–$LiVOPO_4$	$Li_4P_2O_7$	LVP
a (Å)	7.164(10)	8.49942(15)	8.5107(3)	8.6442(12)	6.7671(9)	8.6056
b (Å)	7.000(9)	8.49942(15)	8.6059(3)	7.1002(8)	7.1937(6)	8.5917
c (Å)	7.050(6)	20.8080(6)	11.9437(4)	5.1901(5)	7.9223(9)	12.037
α (°)	90	90	90	111.44	89.950(9)	90
β (°)	90	90	90	89.986	91.223(8)	90.609
γ (°)	90	120	90	103.07	116.957(11)	90
Volume (Å³)	353.6(7)	1301.78(6)	874.78(5)	287.63(6)	343.66(7)	889.93
Space Group	C2221	R-3c	Pbna	P-1	P-1	P21/n
Weight %	1.4	39.16	46.02	12.23	1.19	0